IOP Publishing Semiconductor Science and Technology
Semicond. Sci. Technol. 33 (2018) 104005 (5pp) https://doi.org/10.1088/1361-6641/aaddf0

Ferromagnet/semiconductor/ferromagnet hybrid trilayers grown using solid-phase epitaxy

S Gaucher, B Jenichen and J Herfort

Paul-Drude-Institut für Festkörperelektronik, Leibniz-Institut im Forschungsverbund Berlin e.V., Hausvogteiplatz 5-7, D-10117 Berlin, Germany

E-mail: bernd.jenichen@pdi-berlin.de

Received 11 June 2018, revised 17 August 2018
Accepted for publication 30 August 2018
Published 19 September 2018

Abstract

The direct growth of semiconductors (SC) over metals by molecular beam epitaxy is a difficult task due to the large differences in crystallization energy between these types of materials. This aspect is problematic in the context of spintronics, where coherent spin injection must proceed via ballistic transport through sharp interfacial Schottky barriers. We report the realization of single-crystalline ferromagnet/SC/ferromagnet hybrid trilayers using solid-phase epitaxy, with combinations of Fe_3Si, Co_2FeSi, and Ge. The slow annealing of amorphous Ge over Fe_3Si results in a crystalline film identified as $FeGe_2$. When the annealing is performed over Co_2FeSi, reflected high-energy electron diffraction and x-ray diffraction indicate the creation of a different crystalline Ge(Co,Fe,Si) compound, which also preserves growth orientation. It was possible to observe independent magnetization switching of the ferromagnetic layers in a $Fe_3Si/FeGe_2/Co_2FeSi$ sample, thanks to the different coercive fields of the two metals and to the quality of the interfaces. This result is a step towards the implementation of vertical spin-selective transistor-like devices.

Keywords: semiconductor, ferromagnet, spintronics, heteroepitaxy

1. Introduction

The growth by molecular beam epitaxy (MBE) of ferromagnetic (FM) Heusler alloys and semiconductor (SC) heterostructures was found to be a successful approach to realize a number of applications in the field of spintronics [1, 2]. The possibility to create lattice-matched and sharp FM/SC interfaces is important to realize high spin injection efficiency, as intermixing and ordering effects are known to play a detrimental role on spin transport [3–6]. Since there is a large conductivity mismatch between conventional ferromagnets and SCs, coherence is better preserved when spin injection proceeds via tunneling through a narrow Schottky barrier [7–10], whose profile is also highly influential [11]. Such studies are more easily performed in bilayer systems, where a single-crystalline FM film is grown over a SC substrate by MBE. Indeed, metals usually require lower crystallization temperatures, which ensures that no undesirable mixing or byproducts occur at the SC/FM interface. Growing a SC over a metallic substrate is however more challenging, and can be a limiting factor for a number of envisaged applications, such as vertical spin-selective devices made in the FM/SC/FM configuration.

Ge has been used as a candidate SC to grow on FM surfaces due to its relatively low crystallization temperature (~300 °C), which offers better chances to prevent intermixing at the interface. The growth of Ge over FM Heusler alloys was investigated by MBE [12–15], surfactant-mediated MBE [16, 17] and more recently solid-phase epitaxy (SPE) [18, 19]. Using the latter approach, it was shown that the slow annealing of a thin amorphous Ge film over Fe_3Si can yield a compound identified as $FeGe_2$ [20], over which it was possible to grow another single-crystalline Fe_3Si layer.

In this work, we extend the SPE technique to include Co_2FeSi within the trilayer stacks. Co_2FeSi and Fe_3Si have similar lattice parameters, and thus can both be grown by MBE in a lattice-matched way over GaAs and Ge. The two FM materials are known to have coercive fields differing by

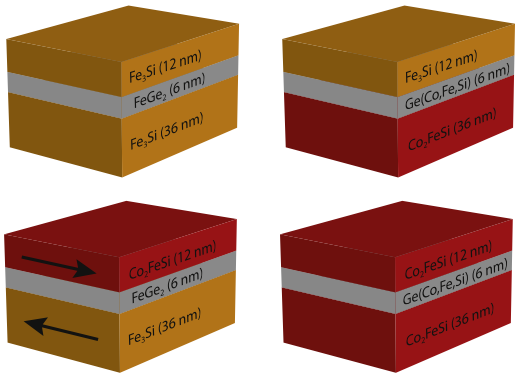

Figure 1. Four trilayer stacking sequences containing a first 36 nm FM layer (Co_2FeSi or Fe_3Si), a 6 nm SC buffer layer (Ge crystallized by annealing), and a capping 12 nm FM layer (Co_2FeSi or Fe_3Si). An objective is to independently control the magnetization of each FM layer as illustrated on the bottom left stack.

only a few Oe [21, 22], which is an advantage to control the magnetization of the films independently. Co_2FeSi has the highest magnetic moment per unit cell and highest Curie temperature of all FM Heusler alloys. It has also for long been expected to exhibit a half-metallic character. Although this property is being disputed, one can minimally expect the compound to offer a degree of spin polarization in the 40%–60% range [23].

Despite the relatively high reactivity of Co_2FeSi (compared to Fe_3Si), it was still possible to use the SPE approach to crystallize amorphous Ge films and achieve fully epitaxial trilayers. The realization of such heterostructures, including FM materials with different coercive fields, is a supplementary step towards the creation of new spin-selective devices that could be operated both as tunnel transistors and magnetic tunnel junctions.

2. Experimental

Figure 1 shows four stacking sequences used in this study, where a Ge buffer layer is inserted between two FM films with thicknesses of 36 and 12 nm. The two FM layers are either Fe_3Si or Co_2FeSi, or a combination of both. The samples are grown using low temperature MBE and SPE, building on methods that were described previously [18]. GaAs(001) substrates are prepared with a 350 nm buffer layer, grown by MBE at 540 °C and As-terminated. The samples then are transferred under UHV into an As-free chamber, in which Fe_3Si and Co_2FeSi layers are grown by co-deposition from high-temperature effusion cells, both at 200 °C. On top of these first FM layers, the equivalent of 6 nm of crystalline Ge is deposited at 150 °C, which in fact results in an amorphous film. The samples are then annealed *in situ* by slowly increasing the temperature (5° min^{-1}) up to 245 °C (over Co_2FeSi) or 260 °C (over Fe_3Si) for 10 min. During the annealing, the crystallization of the amorphous Ge layer is monitored by reflected high-energy electron diffraction (RHEED). The annealing temperatures were determined by observing the appearance of streaks in the RHEED patterns, which confirmed the obtention of crystalline layers. Capping Fe_3Si or Co_2FeSi layers are then grown directly over the crystallized compounds, under the same conditions as the respective first layers.

The structure and quality of the trilayer stacks were evaluated by x-ray diffraction (XRD) using an X-Pert PRO MRD™ system with Cu$K\alpha_1$ radiation source having a wavelength $\lambda = 1.540\,56$ Å. The FM layers are made with thicknesses in a ratio of 3:1 in order for their individual contributions to appear clearly in the XRD patterns (finite thickness oscillations with 1:3 beating pattern). The magnetization of the trilayers was measured in a superconducting quantum interference device (SQUID), using standard AC techniques. For that purpose, the samples were cut into pieces of approximately 3×4 nm and cooled to 10 K.

3. Results

All four hybrid trilayer configurations (illustrated in figure 1) have single-crystalline individual layers that preserve growth orientation. Figure 2 shows a comparison of the RHEED patterns taken during the growth of two samples. In (a), the crystallization the amorphous Ge film is performed over a Fe_3Si surface. The resulting compound is a 2D allotrope of $FeGe_2$ with space group *P4mm* (with a small amount of diffused Si atoms sitting on Ge sites). This material does not exist in a bulk form and results from the minimization of the elastic energy of the epitaxial film [20]. There is a clear distinction between the patterns observed along the [110] and [010] directions. A relationship can thus be established with the orientation of the overgrown Co_2FeSi film, for which the streaks coincide for the same sample alignments. In (b), the annealing is done over a Co_2FeSi surface. Although the exact stoichiometry of the Ge(Co,Fe,Si) film was not determined, the RHEED pattern depicts a lattice-matched compound over which the pseudomorphic growth of Fe_3Si was possible. The absence of Kikuchi lines in the Ge(Co,Fe,Si) images is a sign that the surface is not as flat as the one obtained for $FeGe_2$, a feature that is also noticeable in the XRD curves of those trilayers. Surprisingly, the creation of $FeGe_2$ and Ge(Co,Fe,Si) seems to leave the stoichiometry of the underlying metallic films intact. In recently published studies of similar trilayers [18, 20], high-resolution transmission electron microscopy images show that the crystallinity of the underlying Fe_3Si is unaltered upon annealing of the amorphous Ge, in large regions of perfect and lattice-matched interfaces. Thus, it is assumed that the magnetic properties of the FM films were not degraded during SPE, and that only the roughness of the interfaces plays a noticeable role in the magnetization.

Figure 3 shows the XRD curves of the four samples with different layer combinations. In (a), $FeGe_2$ corresponds to the rounded peaks centered around ∼16.5° and ∼34°, with overlapping Fe_3Si film oscillations. The layered structure of the $FeGe_2$ is a superstructure with a period of two monolayers, which explains the satellite peak at $\omega \sim 25°$ [20]. The Ge(Co,Fe,Si) forming over Co_2FeSi has peaks that coincide

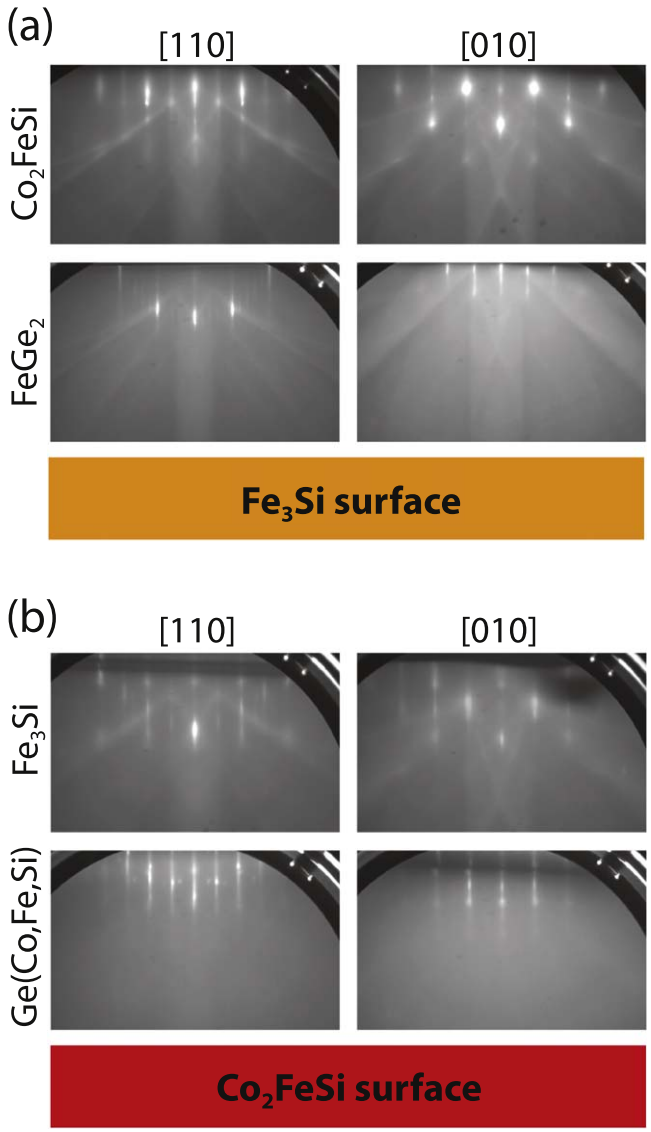

Figure 2. (a) RHEED images taken during the growth of a $Fe_3Si/FeGe_2/Co_2FeSi$ trilayer along the [110] and [010] azimuths. (b) Corresponding RHEED images taken during the growth of a $Co_2FeSi/Ge(Co,Fe,Si)/Fe_3Si$ trilayer. The SPE of amorphous Ge yields different compounds depending on the nature of the underlying surface. It does not prevent the stacks from preserving the same crystal orientation, as seen from the alignment of the streaks of the capping FM films.

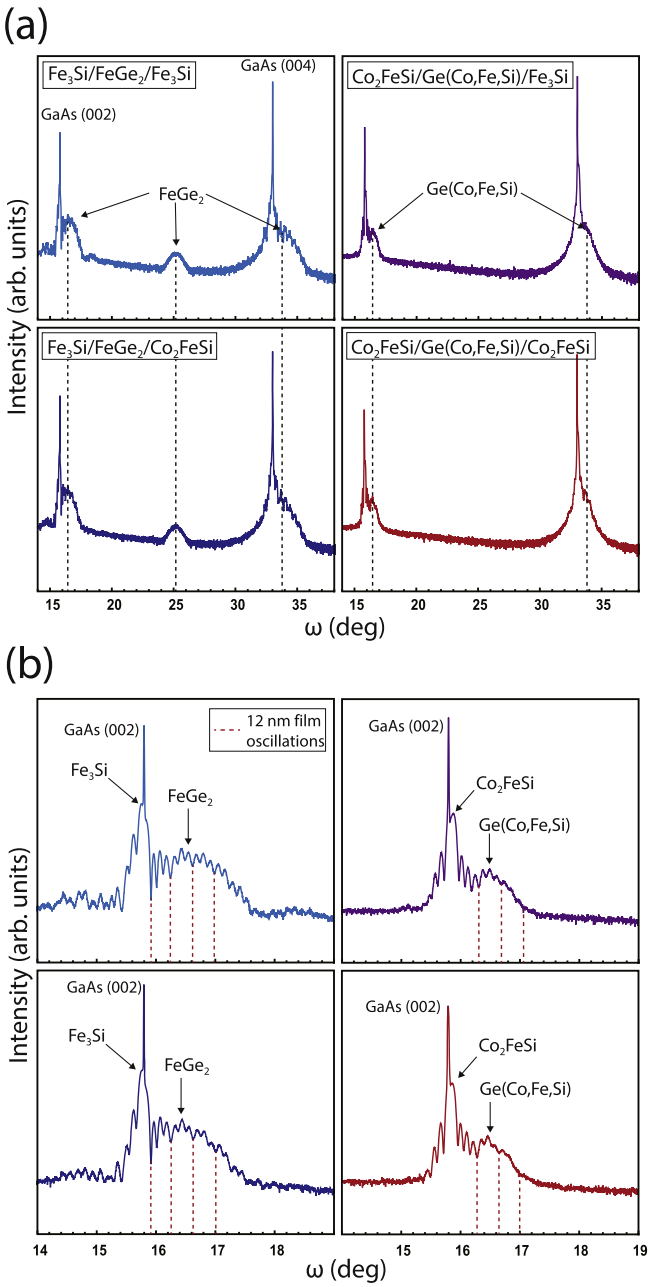

Figure 3. XRD of four trilayer stacks, consisting of different combinations of Fe_3Si, Co_2FeSi and Ge compounds as indicated on each curves (see placement in figure 1). (a) Wide range diffraction curve showing a characteristic $FeGe_2$ peak about $\omega \approx 25°$ for samples with underlying Fe_3Si layer, as well as the crystalline Ge(Co,Fe,Si) peak over Co_2FeSi layers. (b) Close-up of the XRD curves about the GaAs(002) substrate peak, showing a beating pattern in the FM film oscillations.

with the $FeGe_2$ ones. However, it does not have a layered structure, as can be asserted from the absence of a similar satellite peak. Panel (b) shows a close-up of the XRD curves near the GaAs(002) reflection peak. For all four trilayer stacks, it is possible to notice the contribution from both FM layers in the finite thickness oscillations. The 36:12 nm thickness ratio effectively generates a beating pattern between oscillations with periods in a 1:3 ratio. The clarity of these oscillations is better when the SPE is performed over Fe_3Si, which indicates that the stacks have better interface quality. The layered structure of the $FeGe_2$ is likely responsible for the sharpness of the interfaces. Thus, the SPE approach yields crystalline films over both Fe_3Si and Co_2FeSi surfaces, but the quality of the $FM/FeGe_2$ interfaces is better, which is an advantage in order to achieve clear and abrupt magnetization switching.

Figure 4 shows the ideal behavior for the magnetization hysteresis of a trilayer. The sample used for this curve is the $Fe_3Si/FeGe_2/Co_2FeSi$ stack, with external field applied along the easy magnetization axis of the FM films. At high positive field, both Fe_3Si and Co_2FeSi layers are magnetized along the same orientation. As the field is decreased, the magnetization of the thicker Fe_3Si layer flips first, resulting in a plateau. The

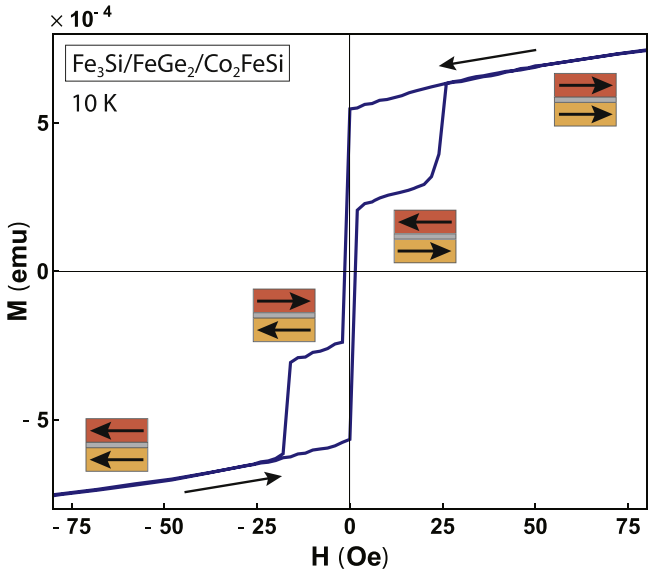

Figure 4. SQUID magnetization hysteresis loops of a $Fe_3Si/FeGe_2/Co_2FeSi$ sample cooled down to 10 K along the easy magnetization axis of the FM films. The curve shows clear intermediary plateaus corresponding to antiparallel magnetization of the Fe_3Si and Co_2FeSi films. The short arrows represent the orientation of the magnetization of the bottom and top films. The long arrows indicate the direction of the hysteresis loop. (The curves were recentered to correct for a known offset in the SQUID setup.)

Co_2FeSi layer then flips at slightly higher negative field, due to the higher coercivity of the material (indicated by bold arrows). Thinner films also tend to have higher coercive fields, which in this case accentuates the effect. A similar sequential switching is observed along the other direction of the hysteresis loop. The contribution to the total magnetization of the $FeGe_2$ film is not observed on this curve. Indeed, one would expect $FeGe_2$ to show ferromagnetism since it contains a FM element. Ongoing SQUID investigations of isolated $FeGe_2$ thin films grown by SPE over GaAs indicate a magnetization about an order of magnitude smaller than Fe_3Si and Co_2FeSi, with much higher coercive field around 200 Oe [24]. $FeGe_2$ can therefore act as an effective layer to decouple the adjacent Fe_3Si and Co_2FeSi films, whose magnetization reversal occurs within a hysteresis loop limited to ± 25 Oe.

It was not possible to observe clear independent magnetic switching of the FM layers using the samples having other stacking orders. The samples with underlying Co_2FeSi have rougher interfaces, which resulted in ill-defined features around the magnetization reversal. Single-crystalline Fe_3Si films have small coercive fields and abrupt magnetization reversal (within 1 Oe). Also, coercivity is known to depend on the thickness of the FM thin films. However, despite having ideal interface quality, the different thickness of the Fe_3Si films (36 and 12 nm) in the $Fe_3Si/FeGe_2/Fe_3Si$ sample did not translate into a sufficiently large coercivity mismatch to resolve plateaus of antiparallel magnetization. The combination of Fe_3Si and Co_2FeSi with $FeGe_2$ buffer layer is therefore the best of all four stacking configurations.

4. Conclusion

The growth of FM/SC/FM trilayer stacks was investigated by a combination of low temperature MBE and SPE. The crystallization of amorphous Ge was successful on both Fe_3Si and Co_2FeSi surfaces. On Fe_3Si, a layered allotrope of $FeGe_2$ arises spontaneously, while another Ge(Co,Fe,Si) compound forms over Co_2FeSi. In both cases, capping Fe_3Si or Co_2FeSi layers could be added by MBE while preserving the same growth orientation, as confirmed by the *in situ* RHEED patterns. XRD revealed the contribution from all three layers, independently of the order in which the layers were grown. However, higher interfacial quality is achieved when SPE is performed over Fe_3Si. Using a $Fe_3Si/FeGe_2/Co_2FeSi$ sample, it was possible to observe clear independent magnetization switching of the FM films. The different thickness and coercive fields of the materials, the quality of the crystalline films, as well as the sharpness of the $FM/FeGe_2$ interfaces are responsible for the appearance of the effect in this specific sample. The successful realization of such hybrid FM/SC/FM trilayers is a step towards the realization of vertical spintronics devices.

Acknowledgments

The authors thank C Herrmann and H-P Schönherr for their support during the growth of the samples.

ORCID iDs

B Jenichen https://orcid.org/0000-0001-5012-1618

References

[1] Palmstrøm C J 2003 *MRS Bull.* **28** 725
[2] Palmstrøm C J 2016 *Prog. Cryst. Growth Charact. Mater.* **62** 371
[3] Schultz B D, Marom N, Naveh D, Lou X, Adelmann C, Strand J, Crowell P A, Kronik L and Palmstrøm C J 2009 *Phys. Rev.* B **80** 201309
[4] Adelmann C, Schultz B D, Dong X Y, Palmstrom C J, Lou X, Strand J, Xie J Q, Park S, Fitzsimmons M R and Crowell P A 2004 *16th IPRM. 2004 Int. Conf. on Indium Phosphide and Related Materials (Kagoshima, Japan, 2004)* p 505
[5] Zega T J, Hanbicki A T, Erwin S C, Žutić I, Kioseoglou G, Li C H, Jonker B T and Stroud R M 2006 *Phys. Rev. Lett.* **96** 196101
[6] Demchenko D O and Liu A Y 2006 *Phys. Rev.* B **73** 115332
[7] Schmidt G, Ferrand D, Molenkamp L W, Filip A T and van Wees B J 2000 *Phys. Rev.* B **62** R4790
[8] Rashba E I 2000 *Phys. Rev.* B **62** R16267–70
[9] Hanbicki A T, Jonker B T, Itskos G, Kioseoglou G and Petrou A 2002 *Appl. Phys. Lett.* **80** 1240
[10] Hanbicki A T, van't Erve O M J, Magno R, Kioseoglou G, Li C H, Jonker B T, Itskos G, Mallory R, Yasar M and Petrou A 2003 *Appl. Phys. Lett.* **82** 4092

[11] Hu Q O, Garlid E S, Crowell P A and Palmstrøm C J 2011 *Phys. Rev.* B **84** 085306
[12] Yamada S, Tanikawa K, Miyao M and Hamaya K 2012 *Cryst. Growth Des.* **12** 4703
[13] Kawano M, Yamada S, Tanikawa K, Sawano K, Miyao M and Hamaya K 2013 *Appl. Phys. Lett.* **102** 121908
[14] Jenichen B, Herfort J, Jahn U, Trampert A and Riechert H 2014 *Thin Solid Films* **556** 120
[15] Hamaya K, Kawano M, Fujita Y, Oki S and Yamada S 2016 *Mater. Trans.* **57** 760–6
[16] Maafa I, Hajjar-Garreau S, Jaafar R, Berling D, Pirri C, Mehdaoui A, Denys E, Florentin A and Garreau G 2013 *J. Phys.: Condens. Matter* **25** 256007
[17] Kawano M, Ikawa M, Arima K, Yamada S, Kanashima T and Hamaya K 2016 *J. Appl. Phys.* **119** 045302
[18] Gaucher S, Jenichen B, Kalt J, Jahn U, Trampert A and Herfort J 2017 *Appl. Phys. Lett.* **110** 102103
[19] Sakai S, Kawano M, Ikawa M, Sato H, Yamada S and Hamaya K 2017 *Semicond. Sci. Technol.* **32** 094005
[20] Jenichen B, Hanke M, Gaucher S, Trampert A, Herfort J, Kirmse H, Haas B, Willinger E, Huang X and Erwin S C 2018 *Phys. Rev. Mater.* **2** 051402
[21] Herfort J, Schönherr H-P, Friedland K-J and Ploog K H 2004 *J. Vac. Sci. Technol.* B **22** 2073
[22] Hashimoto M, Herfort J, Schnherr H-P and Ploog K H 2005 *Appl. Phys. Lett.* **87** 102506
[23] Makinistian L, Faiz M M, Panguluri R P, Balke B, Wurmehl S, Felser C, Albanesi E A, Petukhov A G and Nadgorny B 2013 *Phys. Rev.* B **87** 220402
[24] Gaucher S, Jenichen B and Herfort J unpublished